Compromising the phosphodependent regulation of the $GABA_AR$ β3 subunit reproduces the core phenotypes of autism spectrum disorders

Thuy N. Vien[a], Amit Modgil[a], Armen M. Abramian[a], Rachel Jurd[a], Joshua Walker[a], Nicholas J. Brandon[b], Miho Terunuma[c], Uwe Rudolph[d], Jamie Maguire[a], Paul A. Davies[a], and Stephen J. Moss[a,e,1]

[a]Department of Neuroscience, Tufts University School of Medicine, Boston, MA 02111; [b]AstraZeneca Neuroscience iMed, Cambridge, MA 02139; [c]Department of Cell Physiology and Pharmacology, University of Leicester, Leicester LE1 9HN, United Kingdom; [d]Laboratory of Genetic Neuropharmacology, McLean Hospital, and Department of Psychiatry, Harvard Medical School, Belmont, MA 02478; and [e]Department of Neuroscience, Physiology, and Pharmacology, University College, London WC1E 6BT, United Kingdom

Edited by Richard L. Huganir, The Johns Hopkins University School of Medicine, Baltimore, MD, and approved October 22, 2015 (received for review July 24, 2015)

Alterations in the efficacy of neuronal inhibition mediated by $GABA_A$ receptors ($GABA_ARs$) containing β3 subunits are continually implicated in autism spectrum disorders (ASDs). In vitro, the plasma membrane stability of $GABA_ARs$ is potentiated via phosphorylation of serine residues 408 and 409 (S408/9) in the β3 subunit, an effect that is mimicked by their mutation to alanines. To assess if modifications in β3 subunit expression contribute to ASDs, we have created a mouse in which S408/9 have been mutated to alanines (S408/9A). S408/9A homozygotes exhibited increased phasic, but decreased tonic, inhibition, events that correlated with alterations in the membrane stability and synaptic accumulation of the receptor subtypes that mediate these distinct forms of inhibition. S408/9A mice exhibited alterations in dendritic spine structure, increased repetitive behavior, and decreased social interaction, hallmarks of ASDs. ASDs are frequently comorbid with epilepsy, and consistent with this comorbidity, S408/9A mice exhibited a marked increase in sensitivity to seizures induced by the convulsant kainic acid. To assess the relevance of our studies using S408/9A mice for the pathophysiology of ASDs, we measured S408/9 phosphorylation in *Fmr1* KO mice, a model of fragile X syndrome, the most common monogenetic cause of ASDs. Phosphorylation of S408/9 was selectively and significantly enhanced in *Fmr1* KO mice. Collectively, our results suggest that alterations in phosphorylation and/or activity of β3-containing $GABA_ARs$ may directly contribute to the pathophysiology of ASDs.

GABA receptor | phosphorylation | autism spectrum disorder | tonic inhibition | phasic inhibition

$GABA_A$ receptors ($GABA_ARs$) are Cl^- selective ligand-gated ion channels that mediate phasic and tonic inhibition in the adult brain. Consistent with their roles in limiting neuronal excitability, benzodiazepines, barbiturates, general anesthetics, and neurosteroids exert their anxiolytic, anticonvulsant, hypnotic, and sedative effects via potentiating $GABA_AR$ activity (1). $GABA_ARs$ are heteropentamers constructed from α1–6, β1–3, γ1–3, δ, ε, θ, and π subunits. Phasic inhibition is principally mediated by receptors assembled from α1–3, β1–3, and γ2 subunits, whereas those receptors that mediate tonic inhibition contain α4–6, β1–3, and δ subunits (2). Studies using KO mice have shown that the β3 subunit is an essential component of receptor subtypes that mediate phasic and tonic inhibition (3). Together with the *Fmr1* gene (Fragile X mental retardation), mutations to the 15q11–13 locus, where the $GABA_AR$ β3 gene resides, are the leading monogenetic causes of autism spectrum disorders (ASDs) (4). Moreover, β3 subunit mutations have been described in seizure disorders, and alterations in subunit expression levels have also been reported in ASDs (3, 5).

In vitro studies have revealed that the β3 subunit plays a critical role in regulating the plasma membrane accumulation and synaptic targeting of $GABA_ARs$ via phosphorylation of the intracellular serine residues 408 and 409 (S408/9) (6, 7). S408/9 are substrates of cAMP-dependent PKA, PKC, Ca^{2+}-calmodulin type 2-dependent protein kinases (Cam KIIs), and cGMP-dependent protein kinase, and they are principally dephosphorylated by protein phosphatase 2A (8). S408/9 are the principal mediators of high-affinity binding to the clathrin adaptor molecule AP2 within the β3 subunit, and thereby facilitate $GABA_AR$ endocytosis (9). Phosphorylation of S408/9 reduces the affinity of the β3 subunit for AP2 by 100-fold, and mutation of S408/9 to alanine residues (S408/9A) has been shown to mimic the effects of phosphorylation on AP2 binding to the β3 subunit (9, 10). Accordingly, overexpression of the mutant β3 S408/9A subunit in cultured hippocampal neurons leads to an increase in the number and size of inhibitory synapses (7).

Studies in animal models of ASDs have reported modifications in the expression levels of some $GABA_AR$ mRNAs and proteins (11, 12). However, the mechanisms underlying these alterations in subunit expression and if they contribute to ASDs remain to be addressed. Therefore, in this study, we have analyzed the role that modified β3 subunit phosphorylation may play in the pathophysiology of ASDs. To test this role, we created a

Significance

Alterations in the efficacy of neuronal inhibition mediated by $GABA_A$ receptors ($GABA_ARs$) containing β3 subunits are continually implicated in autism spectrum disorders (ASDs). In vitro, the plasma membrane stability of $GABA_ARs$ is potentiated via phosphorylation of serine residues 408 and 409 (S408/9) in the β3 subunit, an effect that is mimicked by their mutation to alanines. Here, we created a mouse in which S408/9 have been mutated to alanines (S408/9A). S408/9A mice exhibited altered dendritic spine structure, increased repetitive behavior, decreased social interaction, and an epileptic phenotype. Thus, mutation of S408/9 reproduces the core deficits seen in humans with ASDs. Collectively, our results suggest that alterations in phosphorylation and/or activity of β3-containing $GABA_ARs$ may directly contribute to the pathophysiology of ASDs.

Author contributions: T.N.V., A.M., A.M.A., R.J., J.W., M.T., U.R., and J.M. designed research; T.N.V., A.M., A.M.A., R.J., J.W., N.J.B., M.T., U.R., and J.M. performed research; A.M.A., M.T., and U.R. contributed new reagents/analytic tools; T.N.V., A.M., A.M.A., R.J., J.W., N.J.B., M.T., U.R., J.M., and P.A.D. analyzed data; and T.N.V., N.J.B., U.R., J.M., P.A.D., and S.J.M. wrote the paper.

Conflict of interest statement: S.J.M. serves as a consultant for AstraZeneca and SAGE Therapeutics, relationships that are regulated by Tufts University and do not have an impact on this study.

This article is a PNAS Direct Submission.

[1]To whom correspondence should be addressed. Email: stephen.moss@tufts.edu.

This article contains supporting information online at www.pnas.org/lookup/suppl/doi:10.1073/pnas.1514657112/-/DCSupplemental.

mouse in which the principal sites of phosphodependent regulation within the receptor β3 subunit, S408/9, have been mutated to S408/9A, a mutation that mimics the effects of their phosphorylation. S408/9A mice exhibited increased phasic but decreased tonic inhibition events, which correlated with alterations in the membrane stability of the receptor subtypes that mediate these distinct forms of inhibition. S408/9A mice exhibited alterations in dendritic spine structure, increased repetitive-like behavior, and decreased social interaction, which are hallmarks of ASDs. Therefore, our results provide evidence that alterations in the activity of $GABA_A$Rs containing β3 subunits directly contribute to ASDs.

Results

Creation of a S408/9A Knock-In Mouse. Alterations in the efficacy of GABAergic inhibition mediated by β3-containing $GABA_A$Rs are strongly linked to ASDs. Phosphorylation of $GABA_A$Rs regulates their exocytosis and endocytosis, and thereby their residence time on the neuronal plasma membrane and accumulation at inhibitory synapses (8). Central to these regulatory processes is the phosphorylation of S408/9 in the β3 subunit, which reduces the affinity of $GABA_A$Rs for the clathrin adaptor protein AP2, as measured by using synthetic peptides corresponding to the β3 subunit and purified AP2 (9, 13). The significance of these findings has recently been questioned by studies that suggest that the arginine residues flanking S408/9 are the principal determinants of AP2 binding in the β3 subunit (14). To examine the significance of S408/9 further, we expressed the intracellular domain of the β3 subunit as a GST fusion protein (GSTβ3) or a fusion protein in which the respective residues were mutated to alanines (GSTβ3S408/9A) in *Escherichia coli.* The respective fusion proteins were then phosphorylated in vitro using purified PKC to final stoichiometries of ∼0.35 and ∼0.03 mol/mol, respectively, and then exposed to the μ2 subunit of AP2 (15) (Fig. S1*A*). Phosphorylation of GSTβ3 significantly reduced μ2 binding, whereas phosphorylation of GSTβ3S408/9A was without effect. Likewise GSTβ3S408/9A bound significantly lower levels of μ2 compared with GSTβ3. Collectively, these results suggest a key role for S408/9 and their phosphorylation in determining the affinity of $GABA_A$Rs for AP2 (Fig. S1 *A* and *B*).

To assess the significance of β3 subunit phosphorylation in determining the efficacy of GABAergic inhibition, we created a knock-in mouse in which S408/9 were mutated to S408/9A using homologous recombination in ES cells (Fig. S1 *C* and *D*). Mutation of the respective codons in exon 9 of the β3 subunit was confirmed by DNA sequencing (Fig. S1 *C* and *D*), and the respective mice were backcrossed on the C57BL/6J background in excess of 10 generations. S408/9A homozygotes were viable and bred normally and did not exhibit any overt phenotypes. Likewise, there did not appear to be any gross anatomical changes in the structure of the hippocampus (Fig. S1*E*). In hippocampal slices from WT mice, treatment with the PKC activator phorbol 12,13-dibutyrate produced a large increase in pS408/9 immunoreactivity, an effect not replicated in S408/9A mice (Fig. 1*A*). To control for possible global changes in $GABA_A$R phosphorylation mice, we analyzed phosphorylation of Y367 in the γ2 subunit, an accepted substrate of Src family kinases (16). Treatment of slices with vanadate, an inhibitor of tyrosine phosphatases, induced similar increases in Y367 phosphorylation in WT and S408/9A mice (Fig. 1*A*).

Characterization of $GABA_A$R expression levels and synaptic targeting in S408/9A mice. Next, we examined the effects of the S408/9A mutation on the cell surface accumulation of the $GABA_A$Rs using biotinylation. The S408/9A mutation increased the cell surface expression levels of the β3 subunit to 145 ± 8% of WT ($P < 0.05$, $n = 4$ mice of each genotype; Fig. 1*B*) without modifying total subunit expression levels ($P > 0.05$, $n = 4$ mice of each genotype; Fig. 1*C*). In the dentate gyrus, phasic inhibition is mediated by $GABA_A$R assembled from of α1/2, β2, β3, and γ2 subunits, whereas subtypes containing α4–6, β2, β3, and δ subunits are responsible for tonic current. Therefore, we assessed the effects of the S408/9 mutation on the plasma membrane accumulation of the receptor α2 and α4 subunits. The plasma membrane levels of the α2 subunit were increased in S408/9A mice to 119.0 ± 5.2% of control ($P < 0.05$, $n = 5$–6 mice of each genotype; Fig. 1*B*). In

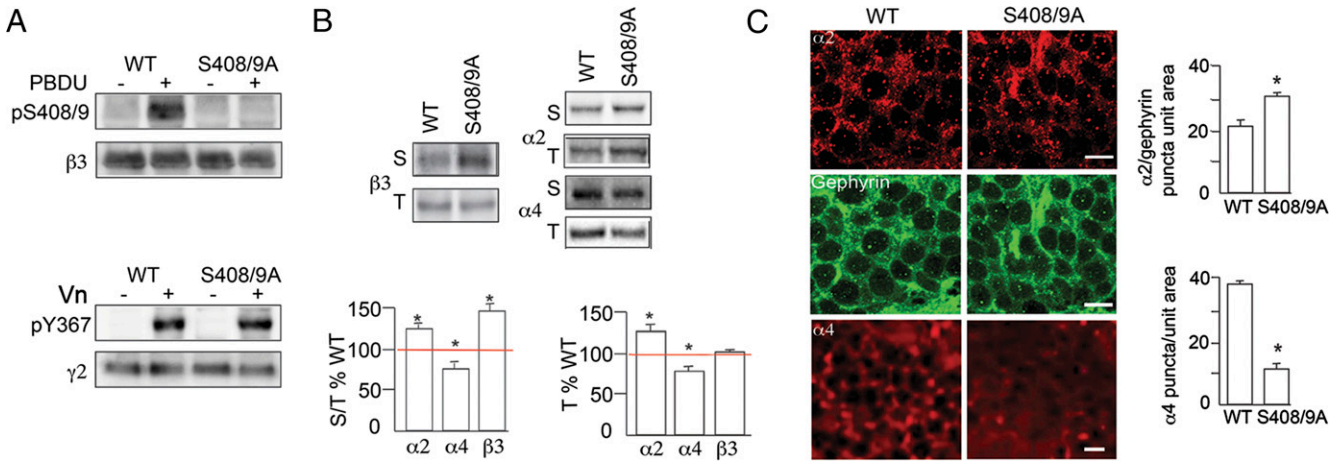

Fig. 1. $GABA_A$R expression in S408/9A mice. (*A*) Treatment of hippocampal slices from WT mice with 100 nM phorbol 12,13-dibutyrate (PDBU) increased pS408/9 immunoreactivity consistent with published studies demonstrating that both residues are substrates of PKC (8). In contrast, pS408/9 immunoreactivity was not detected in S408/9A mice. (*B*) Biotinylation revealed that the surface levels of the β3 subunits, along with the synaptic α2 subunits, were increased in the S408/9A mice, whereas surface accumulation of $GABA_A$Rs containing α4 subunits was decreased. Hippocampal slices were subjected to biotinylation, followed by immunoblotting with anti-α2, anti-α4, and anti-β3 subunit antibodies. The ratio of surface/total (S/T%WT) was measured in S408/9A mice and WT control mice, and values were then normalized to WT controls (100%, red line). Total expression levels were also compared between genotypes (T%WT). *Significantly different from control ($P < 0.05$, *t* test; $n = 5$–6 mice of each genotype). (*C*) Forty-micron hippocampal slices were stained with antibodies against the α2 and α4 subunits and gephyrin fluorescent-conjugated secondary antibodies, followed by confocal microscopy. The number of α2/gephyrin-positive puncta and α4 puncta was then compared within the dentate gyrus between genotypes. Preventing phosphorylation of the β3 subunit increases the number of inhibitory synapses in the dentate gyrus of the hippocampus but reduces α4 puncta immunoreactivity. *Significantly different from control ($P < 0.001$, *t* test; $n = 3$ mice of each genotype). (Scale bars: 10 μm.)

contrast, the α4 subunit was decreased to 81.0 ± 4.5% of levels seen in WT ($P < 0.05$, $n = 6$ mice of each genotype; Fig. 1*B*). These changes in cell surface accumulation were mirrored by parallel changes in increased total expression levels of the α2 subunits and decreased total expression levels of the α4 subunits to 120.7 ± 4.3% and 85.3 ± 7.0%, respectively, compared with WT controls ($P < 0.05$, $n = 4$–8 mice of each genotype; Fig. 1*B*).

To characterize the subcellular distribution of $GABA_A$Rs in S408/9A mice, hippocampal sections were subjected to immunohistochemistry with antibodies against $GABA_A$R α2 or α4 subunits. In some experiments, sections were also stained with antibodies against the inhibitory scaffold protein gephyrin. Sections were then visualized using confocal microscopy, and subunit expression levels were quantified within the dentate gyrus. The number of inhibitory synapses defined as α2/gephyrin puncta were increased in S408/9A mice compared with WT littermates (23.4 ± 2.5 vs. 32.0 ± 0.6 for WT and S408/9A mice, respectively; $P < 0.05$, $n = 3$ mice of each genotype; Fig. 1*C*). In contrast, the number of puncta of α4 subunit immunoreactivity was decreased (13.1 ± 1.2 vs. to 37.4 ± 0.8 puncta per 2,500 μm^2 for S408/9A and WT mice, respectively; $P < 0.001$; Fig. 1*C*). Additionally, in contrast to the effects seen with $GABA_A$Rs, the levels of gephyrin, postsynaptic density protein-95, and the AMPA receptor subunit GluA1 were unaffected by the S408/9A mutation (Fig. S2).

Collectively, these results reveal that S408/9A mice have deficits in the cell surface accumulation of $GABA_A$Rs that mediate tonic inhibition but an increased level of those $GABA_A$Rs that mediate phasic inhibition.

S408/9A exhibited an increase in phasic inhibition and decreased tonic current. To examine the functional significance of the alterations in $GABA_A$R expression seen in S408/9A mice, we used patch-clamp recording to analyze GABAergic inhibition in dentate gyrus granule cells (DGGCs). In DGGCs from S408/9A mice, tonic current was significantly decreased (24.7 ± 4.1 vs. 11.9 ± 2.2 pA for WT and S408/9A mice, respectively; $P < 0.005$, $n = 10$–11 cells, three mice of each genotype; Fig. 2*A*). In contrast, the amplitude of spontaneous inhibitory postsynaptic currents (sIPSCs) was significantly increased in S408/9A mice compared with WT controls (28.4 ± 2.4 vs. 42.5 ± 3.3 pA for WT and S408/9A mice, respectively; $P < 0.005$, $n = 17$–18 cells, three mice of each genotype; Fig. 2*B*). However, the frequency (4.5 ± 0.2 vs. 4.4 ± 0.1 Hz for WT and S408/9A mice, respectively) and decay time (44.7 ± 12.8 vs. 24.8 ± 2.5 ms for WT and S408/9A mice, respectively; $P > 0.05$, $n = 17$–18 cells, three mice of each genotype) of sIPSCs was comparable between genotypes.

We also assessed the impact of the modifications in GABAergic inhibition on neuronal excitability. First, we compared the properties of excitatory postsynaptic currents (EPSCs) in DGGCs. In S408/9A mice, EPSC amplitude was significantly increased (14.6 ± 1.05 vs. 18 ± 1.02 pA for WT and S408/9A mice, respectively; $P < 0.05$; Fig. 2*C*) with no difference in frequency (1.4 ± 0.3 vs. 1.3 ± 0.2 Hz for WT and S408/9A mice, respectively). Moreover, their decay was also prolonged (2.1 ± 0.1 vs. 2.4 ± 0.2 ms for WT and S408/9A mice, respectively; $P < 0.05$, $n =$ 14–16 cells, three mice of each genotype). However, net excitability of DGGCs and their resting membrane potentials were not modified by the S408/9A mutation ($n = 19$–20 cells, three mice of each genotype; Fig. 2*D* and Table S1).

Therefore, S408/9A mice have reduced tonic but enhanced phasic inhibition, but these changes do not lead to any gross changes in neuronal excitability, presumably because S408/9A mice also exhibit elevations in EPSC amplitude.

S408/9A Mice Exhibit Deficits in Social Interaction and Increased Repetitive Behavior. ASDs have a common core of behavioral deficits, including reduced social interaction and increased repetitive behavior. Therefore, we assessed if any of these parameters are altered in S408/9A mice. First, we assessed if the respective mutation modifies motor coordination as measured using the rotarod, a critical control for data interpretation in rodent behavioral experiments. The latency to fall in the rotarod test was not different at 16–32 rpm in S408/9A mice compared with WT mice (Fig. S3*A*). Likewise, there were no differences between genotypes for the total distance traveled or dwell time in the center of the open field (Fig. S3 *B* and *C*). We also compared anxiety-like behavior using the light/dark test. WT and S408/9A mice spent equivalent time in the light chamber (46.9 ± 2.2% vs. 41.8 ± 2.5% for WT and S408/9A mice, respectively; $P > 0.05$, $n = 12$ mice of each genotype; Fig. S3*D*).

Social behavior was measured using the two-choice and three-chamber social interaction test. In the two-choice assay, WT controls spent more time in the chamber containing the novel mouse than in the chamber containing the empty cage, whereas S408/9A mice had no preference for the novel mouse over the

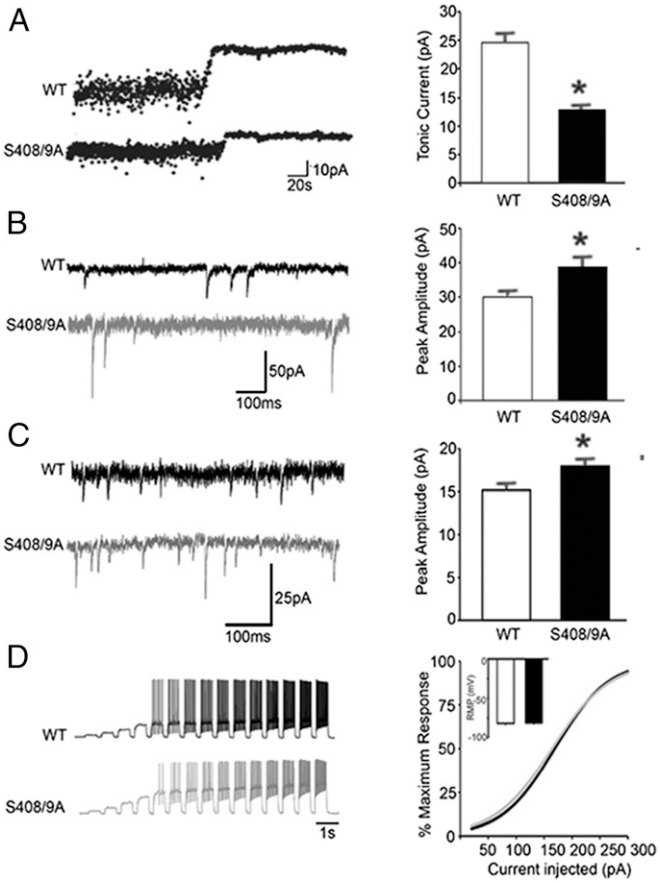

Fig. 2. Characterization of phasic and tonic inhibition in S408/9A mice. (*A*) Tonic conduction is decreased in S408/9A mice. Tonic current in DGGCs was compared between genotypes in the presence and absence of gabazine. The tonic current amplitude of S408/9A mice was significantly smaller than tonic current amplitude of WT mice. *Significantly different from control ($P < 0.01$, *t* test; $n = 10$–11 cells, three mice of each genotype). (*B*) sIPSCs were recorded from DGGCs of WT mice (black) and S408/9A mice (gray) *Significantly different from WT control ($P < 0.001$, *t* test; $n = 17$–18 cells, three mice of each genotype). (*C*) Examples of EPSCs recorded from DGGCs of WT mice (black) and S408/9A mice (gray) *Significantly different from control ($P <$ 0.05, *t* test; $n = 14$–16 cells, three mice of each genotype). (*D*) Representative recordings of action potential firing in DGGCs from WT mice (black) and S408/9A mice (gray) in response to 0.5-s current injections from 20 to 300 pA in 20-pA increments. Average input/output curves from DGGCs from WT mice (black) and S408/9A mice (gray) are shown as a Boltzmann function generated by the averages of the fitted parameters. (*Inset*) No difference in the resting membrane potential (RMP) was observed between genotypes. Values are mean ± SEM ($n = 19$–21 cells, three mice of each genotype).

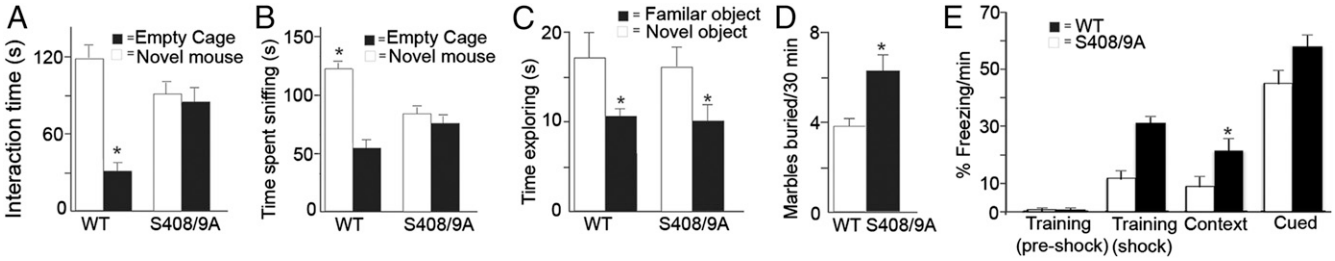

Fig. 3. Characterization of social interaction and repetitive-like behavior in S408/9A mice. (*A*) Preference for an empty cage or novel mouse was determined in a two-choice social interaction setup. *Significantly different from control ($P < 0.01$, ANOVA with Tukey's post hoc comparison; $n = 12$ mice of each genotype). (*B*) Three-chamber social interaction assay was used to measure the preference for a novel mouse or an empty cage. The amount of time mice spent in a predefined sniffing zone around the empty cage or novel mouse was digitally tracked. *Significantly different from control ($P < 0.001$, ANOVA with Tukey's post hoc comparison; $n = 12$–16 mice of each genotype). (*C*) Preference for a familiar object or a novel object was determined for the genotypes. *Significantly different from control ($P < 0.05$, ANOVA with Tukey's post hoc comparison; $n = 10$–12 mice of each genotype). (*D*) Repetitive-like behavior was assessed using the marble burying assay. ($P < 0.01$, *t* test; $n = 18$–19 mice of each genotype). (*E*) Learning and memory were assessed using the fear-conditioning assay. The percentage of freezing per minute was assessed during training and for context-dependent and cued-dependent learning. *Significantly different from control ($P < 0.05$, *t* test; $n = 12$–13 mice of each genotype).

empty cage (time spent interacting with empty cage: 49.8 ± 7.4 s (WT), 86.6 ± 17.6 s (S408/9A); time spent interacting with novel mouse: 119.4 ± 19.0 s (WT), 92.7 ± 17.7 s (S408/9A); $n = 12$ mice of each genotype, $P < 0.01$; Fig. 3*A*). Consistent with the profound deficits in social interaction observed in the two-choice assay, S408/9A mice exhibited no preference for the novel mouse in the three-chamber social interaction assay. WT controls spent more time in the novel mouse sniffing zone than in the empty cage sniffing zone (time spent interacting with empty cage: 55.4 ± 5.8 s (WT), 71.9 ± 8.4 s (S408/9A); time spent interacting with novel mouse: 123.8 ± 5.1 s (WT), 85.7 ± 6.9 s (S408/9A); $n = 12$–16 mice of each genotype, $P < 0.01$; Fig. 3*B*). In contrast, S408/9A mice showed no preference for the novel mouse over an empty cage, consistent with ASD-like deficits in social interaction. As a control for our measurements for social preference, we examined the ability of S408/9A mice to discriminate between a novel object and a familiar object. Both WT controls and S408/9A mice spent more time interacting with the novel object (66 ± 0.9% vs. 64 ± 7.7% of total time for WT and S408/9A mice, respectively; $P < 0.05$, $n = 10$–11 mice of each genotype; Fig. 3*C*).

To measure repetitive-like behavior in S408/9A mice, we used the marble burying assay. S408/9A mice displayed an increase in repetitive-like behavior in the marble burying test (6.0 ± 0.6 marbles in 30 min compared with 3.8 ± 0.5 marbles in WT controls; $P < 0.001$, $n = 18$–19 mice of each genotype; Fig. 3*D*). Therefore, S408/9A mice exhibited an increase in repetitive-like behavior and deficits in social interaction, which are behavioral characteristics commonly observed in ASDs.

Finally, we assessed if the S408/9A mutation has an impact on cognition by comparing contextual and cued fear conditioning between genotypes. S408/9A mice exhibited enhanced context-dependent learning (training: 11.8 ± 3.0% freezing per minute (WT), 32.1 ± 4.3% freezing per minute (S408/9A); $P > 0.05$; context: 8.9 ± 3.4% freezing per minute (WT), 21.4 ± 4.2% freezing per minute (S408/9A); $P < 0.05$; Fig. 3*E*) compared with WT controls but no statistical differences in cue-dependent learning (cued: 45.1 ± 6.6% freezing per minute (WT), 60.8 ± 6.4% freezing per minute (S408/9A); $P > 0.05$; Fig. 3*E*).

S408/9A Mice Have Increased Seizure Susceptibility. ASDs are frequently comorbid with epilepsy. Therefore, we analyzed the impact of the S408/9A mutation on seizure susceptibility. Mice were implanted with EEG electrodes, and seizures were induced with 20 mg/kg of kainic acid and monitored to ensure seizures reached stage 3–4 on the Racine scale (forelimb clonus and rearing with forelimb clonus). Representative EEG traces during epileptiform events captured 30 min after kainic acid injection illustrate a marked increase in epileptiform activity in S408/9A mice over WT controls (Fig. 4*A*). Strikingly, S408/9A mice exhibited a faster onset to the first epileptiform event compared with WT mice (4.6 ± 0.7 vs. 11.2 ± 1.1 min of latency for S408/9A and WT mice, respectively; $P < 0.001$, $n = 8$–10 mice of each genotype; Fig. 4*B*). Additionally, S408/9A mice entered status epilepticus at an earlier time point than WT controls (41.8 ± 4.3 vs. 61.5 ± 8.6 min for S408/9A and WT mice, respectively; $P < 0.05$, $n = 8$–10 mice of each genotype; Fig. 4*B*). Furthermore, S408/9A mice spent a greater percentage of the total time experiencing epileptiform activity compared with WT controls (82.5 ± 2.1% vs. 65.4 ± 6.4% for S408/9A and WT mice, respectively; $P < 0.05$, $n = 8$–10 mice of each genotype; Fig. 4*B*). Therefore, the S408/9A mutation significantly increases seizure susceptibility.

S408/9A Mice Exhibited Increased Hippocampal Dendritic Spine Density. Alterations in spine structure are a common feature in ASDs (17). Therefore, we assessed if the alterations in GABAergic inhibition have an impact on dendritic structure. Brains from both genotypes were subjected to Golgi staining and visualized using stereology. We quantified the density of spines along 30-μm-long sections of

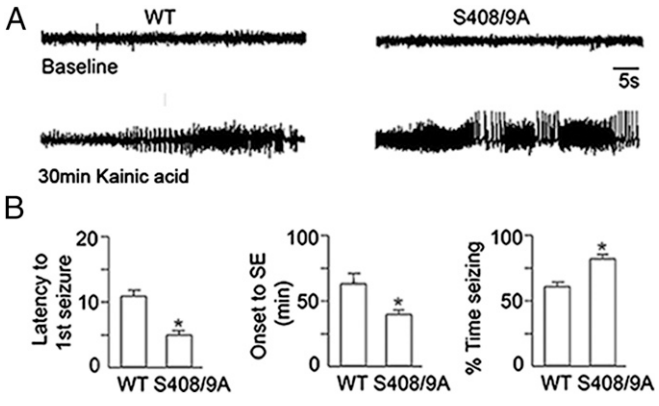

Fig. 4. Characterization of seizure susceptibility in S408/9A mice. (*A*) Representative EEG traces for WT and S408/9A mice at baseline and 30 min after kainic acid injection. (*B*) Latency to the first epileptiform activity, onset of status epilepticus (SE), and total time experiencing epileptiform activity were digitally tracked and measured. S408/9A mice had a shorter latency to the first epileptiform activity, faster onset of status epilepticus, and spent a great percentage of time experiencing epileptiform activity compared with WT controls. *Significantly different from control ($P < 0.05$, *t* test; $n = 8$–10 mice of each genotype).

dendrites in the molecular layer above the dentate gyrus of the hippocampus. In S408/9A mice, a pronounced increase in spine density was seen (28.6 ± 0.7 vs. 34.8 ± 1.0 per 30-μm dendrite for WT and S408/9A mice, respectively; $P < 0.0001$, $n = 12$ neurons in three independent experiments; Fig. 5*A*). Similarly, the spines in S408/9A mice appeared to be more filopodia-like in structure compared with their equivalents in WT mice, and some exhibited pronounced branching. Therefore, S408/9A mice displayed similar abnormalities in spine structure to those abnormalities reported in *Fmr1* KO mice and patients with ASDs.

S408/9A Phosphorylation Is Increased in *Fmr1* KO (Fragile X Syndrome) Mice. To assess the relevance of our studies further, we measured S408/9 phosphorylation in *Fmr1* KO mice, a model of Fragile X syndrome (FXS). S408/9 phosphorylation was significantly increased to 285.6 ± 24.3% in *Fmr1* KO mice compared with WT controls ($P < 0.005$; $n = 3$ mice of each genotype; Fig. 5*B*). In contrast to S408/9, phosphorylation of S383 was similar in *Fmr1* KO mice compared with WT controls ($P > 0.05$, $n = 3$ mice of each genotype; Fig. 5*B*).

Discussion

Deficits in the efficacy of neuronal inhibition mediated by $GABA_A$Rs containing the β3 subunit are widely believed to contribute to the pathophysiology of ASDs. Accordingly, modifications in $GABA_A$R β3 subunit gene structure and/or protein expression levels, together with both deletions and duplications of the 15q11–13 locus, are leading causes of ASDs (5, 18).

In vitro studies have shown that phosphorylation of S408/9 regulates the cell surface stability and synaptic accumulation of β3-containing $GABA_A$Rs (7), and, here, we have analyzed the significance of this putative regulatory process for the pathophysiology of ASDs. To do so, we created a S408/9A knock-in mouse using homologous recombination. S408/9A mice were viable and did not exhibit any overt phenotypes or gross alterations in the structure of the hippocampus. Consistent with the lowered affinity for AP2 in the S408/9A mutation in vitro, the cell surface expression levels of the β3 subunit in the hippocampus were increased in S408/9A mice compared with WT controls. Within the dentate gyrus, the β3 subunit assembles with the α2/γ2 or α4/δ subunits to form $GABA_A$R subtypes that mediate phasic and tonic inhibition, respectively (2). Strikingly, in the dentate gyrus of S408/9A mice, there was a significant increase in the expression levels of the α2 subunit and the number of inhibitory synapses. In contrast, deficits in the expression levels of the α4 subunit were seen. Thus, in addition to membrane trafficking, S408/9 and/or their phosphorylation may play a role in regulating the assembly of individual $GABA_A$R subtypes. Significantly, our findings of alterations in α4 and β3 subunit expression are consistent with GABAergic dysfunction in *Mecp2* and *Fmr1* KO mice, which are accepted models of ASDs (11, 19, 20).

Consistent with this result, the amplitude of sIPSCs was increased and their decay was slowed in DGGCs from S408/9A mice. In contrast, a reciprocal decrease in the cell surface accumulation of the α4 subunit was seen in S408/9A mice, which paralleled a reduction in tonic current. The gross excitability of DGGCs as measured by current injection was not altered between strains, reflecting the increase in EPSC amplitude in S408/9A mice. Therefore, preventing the phosphodependent modulation of the $GABA_A$Rs by mutating S408/9 in the β3 subunit to alanines alters the equilibrium between phasic and tonic inhibition in the dentate gyrus.

Previous in vitro studies have suggested that for synaptic $GABA_A$Rs containing α1/2β3γ2 subunits, mutation of S408/9A does not compromise receptor assembly, or transport to the plasma membrane, but selectively reduces their endocytosis (9). Therefore, the increased synaptic accumulation of the α2 subunit in S408/9A mice presumably results from their enhanced residence time on the plasma membrane. In contrast to synaptic receptors, the mechanisms that control the membrane trafficking of receptors containing α4 subunits are less well defined. However, it is evident from our results that phosphorylation of S408/9 may play opposing roles in regulating the assembly and membrane trafficking of α4 subunit containing $GABA_A$Rs to those roles established for subtypes that mediate phasic inhibition. Clearly, further studies are required to identify the role that S408/9 and their phosphorylation plays in regulating the differential membrane trafficking of $GABA_A$R subtypes that mediate phasic and tonic inhibition.

In parallel with these modifications in GABAergic inhibition, the number of dendritic spines was strikingly increased in the mutant mice. Significantly, overexpressing S408/9A cDNA in cultured hippocampal neurons leads to similar changes in spine maturity to those changes seen in S408/9A mice (7). It is emerging that tonic inhibition plays a central role in reducing neuronal excitability, particularly at depolarizing membrane potentials (21). Given the emerging role for tonic inhibition in regulating neuronal output, the deficits in the efficacy of this process in S408/9A mice may lead to prolonged neuronal depolarization and enhanced intracellular Ca^{2+} signaling, which would be predicted to have significant effects on spine architecture.

In addition to modifications in dendritic structure, ASDs have a common core of behavioral symptoms, including increased repetitive behavior and anxiety, together with deficits in social interaction (17). Therefore, we compared these parameters between genotypes. Compared with WT controls, S408/9A mice exhibited decreased social interaction as measured in both the two-choice and three-chamber assays; however, S408/9A mice and WT controls

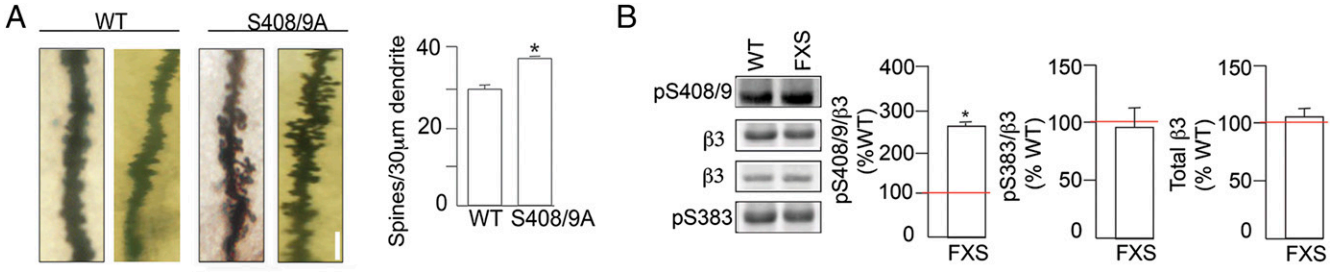

Fig. 5. Characterization of dendritic spine density in DGGCs from S408/9A mice and β3 phosphorylation in *Fmr1* KO (FXS) mice. (*A*) Representative dendrites from DGGCs of two different mice. (Scale bar: 2 μm.) The number of spines per 30 μm of dendrite was then determined and compared between genotypes. *Significantly different from control ($n = 12$ neurons from three independent experiments, three mice of each genotype; $P < 0.0001$, *t* test). (*B*) Hippocampal lysates from WT and *Fmr1* KO mice on a FVB/N (Friend leukemia virus B strain) background were subjected to SDS/PAGE and immunoblotted with pS408/9, pS383, and β3 subunit antibodies. The pS408/9/β3 or pS383/β3 ratios in *Fmr1* KO mice (FXS) were normalized to WT controls (100%; red line). *Significantly different from control ($P < 0.01$, *t* test; $n = 3$ mice of each genotype).

shared a similar preference for a novel object over a familiar object. S408/9A mice also exhibited an increase in repetitive-like behavior as measured using the marble burying assay. Significantly, the mutation did not alter locomotor activity, behavior in the open field, or behavior in the light/dark test. S408/9A mice did not appear to exhibit any modifications in anxiety. ASDs are often comorbid with epilepsy, and consistent with this comorbidity, S408/9A mice exhibit increased sensitivity to kainate-induced seizures. Thus, although the changes in phasic and tonic inhibition seen in S408/9A mice do not appear to lead to changes in net neuronal excitability, they are important determinants of epileptogenesis. Finally, we noted that in the *Fmr1* KO mouse model of FXS, specific alterations in S408/9 phosphorylation were seen. The mechanism linking deficits in FMRP expression and enhanced S408/9 phosphorylation requires further experimentation. However, it is interesting to note that FMRP is part of a signaling complex that contains protein phosphatase 2A (PP2A), the principle phosphatase that dephosphorylates S408/9 (10, 22, 23). Thus, deficits in FMRP expression levels may affect the stability and/or subcellular targeting of PP2A, leading to reduced rates of S408/9 dephosphorylation.

In conclusion, our results suggest that alterations in the phosphorylation status of $GABA_AR$ β3 resulting in compromised GABAergic inhibition are central to the pathophysiology of FXS. Therefore, restoring the efficacy of tonic inhibition may be a useful therapeutic strategy to alleviate the burdens of ASDs.

Materials and Methods

All protocols were approved by Tufts University's Institutional Animal Care and Use Committee and were conducted in accordance with the NIH *Guide for the Care and Use of Laboratory Animals* (24). More detailed information on materials and methods is provided in *SI Materials and Methods*.

Creation of the S408/9A Mice. The S408/9A mice were created using homologous recombination as detailed previously (25).

Biochemical Measurements. Antibodies used in this study have been described previously, as have the methods for immunoblotting and immunoprecipitation (22, 26).

Electrophysiology and EEG Recordings. Phasic and tonic inhibition was measured using the patch-clamp technique (27). The Pinnacle Technology system and LabChart (ADInstruments) were used for EEG recordings and analysis as previously described (28).

Behavior. Measurements using the rotarod and activity in the open field and anxiety were assessed as described previously (26).

ACKNOWLEDGMENTS. We thank Jay Boltax and Hew Mun Lau (McLean Hospital) for technical assistance in generating the mutant allele in ES cells. This work was supported by Grant 206026 from the Simons Foundation (to S.J.M.); NIH–National Institute of Neurological Disorders and Stroke Grants NS051195, NS056359, NS081735, R21NS080064, and NS087662 (to S.J.M.); NIH–National Institute of Mental Health Grant MH097446 (to P.A.D. and S.J.M.); and US Department of Defense Grant AR140209 (to P.A.D. and S.J.M.). J.M. is supported by Grant NS073574, and U.R. is supported by Grant R01MH080006.

1. Rudolph U, Möhler H (2006) GABA-based therapeutic approaches: GABAA receptor subtype functions. *Curr Opin Pharmacol* 6(1):18–23.
2. Brickley SG, Mody I (2012) Extrasynaptic GABA(A) receptors: Their function in the CNS and implications for disease. *Neuron* 73(1):23–34.
3. DeLorey TM, et al. (1998) Mice lacking the beta3 subunit of the GABAA receptor have the epilepsy phenotype and many of the behavioral characteristics of Angelman syndrome. *J Neurosci* 18(20):8505–8514.
4. Abrahams BS, Geschwind DH (2008) Advances in autism genetics: On the threshold of a new neurobiology. *Nat Rev Genet* 9(5):341–355.
5. Delahanty RJ, et al. (2011) Maternal transmission of a rare GABRB3 signal peptide variant is associated with autism. *Mol Psychiatry* 16(1):86–96.
6. Brandon NJ, et al. (1999) Synaptic targeting and regulation of GABA(A) receptors. *Biochem Soc Trans* 27(4):527–530.
7. Jacob TC, et al. (2009) GABA(A) receptor membrane trafficking regulates spine maturity. *Proc Natl Acad Sci USA* 106(30):12500–12505.
8. Nakamura Y, Darnieder LM, Deeb TZ, Moss SJ (2015) Regulation of GABAARs by phosphorylation. *Adv Pharmacol* 72:97–146.
9. Kittler JT, et al. (2005) Phospho-dependent binding of the clathrin AP2 adaptor complex to GABAA receptors regulates the efficacy of inhibitory synaptic transmission. *Proc Natl Acad Sci USA* 102(41):14871–14876.
10. Terunuma M, et al. (2008) Deficits in phosphorylation of GABA(A) receptors by intimately associated protein kinase C activity underlie compromised synaptic inhibition during status epilepticus. *J Neurosci* 28(2):376–384.
11. Martin BS, Corbin JG, Huntsman MM (2014) Deficient tonic GABAergic conductance and synaptic balance in the fragile X syndrome amygdala. *J Neurophysiol* 112(4):890–902.
12. DeLorey TM (2005) GABRB3 gene deficient mice: A potential model of autism spectrum disorder. *Int Rev Neurobiol* 71:359–382.
13. Jacob TC, Moss SJ, Jurd R (2008) GABA(A) receptor trafficking and its role in the dynamic modulation of neuronal inhibition. *Nat Rev Neurosci* 9(5):331–343.
14. Smith KR, et al. (2012) Stabilization of GABA(A) receptors at endocytic zones is mediated by an AP2 binding motif within the GABA(A) receptor β3 subunit. *J Neurosci* 32(7):2485–2498.
15. Moss SJ, Doherty CA, Huganir RL (1992) Identification of the cAMP-dependent protein kinase and protein kinase C phosphorylation sites within the major intracellular domains of the beta 1, gamma 2S, and gamma 2L subunits of the gamma-aminobutyric acid type A receptor. *J Biol Chem* 267(20):14470–14476.
16. Jurd R, Tretter V, Walker J, Brandon NJ, Moss SJ (2010) Fyn kinase contributes to tyrosine phosphorylation of the GABA(A) receptor gamma2 subunit. *Mol Cell Neurosci* 44(2):129–134.
17. Hutsler JJ, Zhang H (2010) Increased dendritic spine densities on cortical projection neurons in autism spectrum disorders. *Brain Res* 1309:83–94.
18. Kang JQ, Barnes G (2013) A common susceptibility factor of both autism and epilepsy: Functional deficiency of GABA A receptors. *J Autism Dev Disord* 43(1):68–79.
19. Olmos-Serrano JL, et al. (2010) Defective GABAergic neurotransmission and pharmacological rescue of neuronal hyperexcitability in the amygdala in a mouse model of fragile X syndrome. *J Neurosci* 30(29):9929–9938.
20. Chao HT, et al. (2010) Dysfunction in GABA signalling mediates autism-like stereotypies and Rett syndrome phenotypes. *Nature* 468(7321):263–269.
21. Wlodarczyk AI, et al. (2013) Tonic GABAA conductance decreases membrane time constant and increases EPSP-spike precision in hippocampal pyramidal neurons. *Front Neural Circuits* 7:205.
22. Jovanovic JN, Thomas P, Kittler JT, Smart TG, Moss SJ (2004) Brain-derived neurotrophic factor modulates fast synaptic inhibition by regulating GABA(A) receptor phosphorylation, activity, and cell-surface stability. *J Neurosci* 24(2):522–530.
23. Narayanan U, et al. (2007) FMRP phosphorylation reveals an immediate-early signaling pathway triggered by group I mGluR and mediated by PP2A. *J Neurosci* 27(52):14349–14357.
24. Committee on Care and Use of Laboratory Animals (1996) *Guide for the Care and Use of Laboratory Animals* (Natl Inst Health, Bethesda), DHHS Publ No (NIH) 85-23.
25. Terunuma M, et al. (2014) Postsynaptic GABAB receptor activity regulates excitatory neuronal architecture and spatial memory. *J Neurosci* 34(3):804–816.
26. Tretter V, et al. (2009) Deficits in spatial memory correlate with modified gamma-aminobutyric acid type A receptor tyrosine phosphorylation in the hippocampus. *Proc Natl Acad Sci USA* 106(47):20039–20044.
27. Kretschmannova K, et al. (2013) Enhanced tonic inhibition influences the hypnotic and amnestic actions of the intravenous anesthetics etomidate and propofol. *J Neurosci* 33(17):7264–7273.
28. Lee V, Maguire J (2013) Impact of inhibitory constraint of interneurons on neuronal excitability. *J Neurophysiol* 110(11):2520–2535.